

A modeling system for tidally driven long-term morphodynamics

ANDRÉ B. FORTUNATO* and ANABELA OLIVEIRA†, *Research Officer, National Civil Engineering Laboratory, Estuaries and Coastal Zones Division, Av. do Brasil, 101, 1700-066 Lisbon, Portugal*

*Corresponding author. E-mail: afortunato@lnec.pt

†E-mail: aoliveira@lnec.pt

ABSTRACT

A modeling system to simulate tidally driven morphodynamics is developed and assessed. The system couples an existing shallow water model with a new morphological updating model. Four innovative features to improve the accuracy and efficiency of the system are implemented and tested. First, two alternatives are proposed to update the velocity field without running the hydrodynamic model. Both alternatives, based on an assumption on the behavior of friction, are more accurate than the traditional “continuity correction”. Second, hydrodynamic results are provided in the frequency domain. The harmonic synthesis of the velocity time series simplifies interpolation and extrapolation of the hydrodynamic model results and the use of different time steps for the various components of the modeling system. Third, the time-integration of the sediment fluxes is performed with a Runge-Kutta method so the time step adapts in space and time to the flow characteristics. Finally, a criterion to determine the need for a new hydrodynamic simulation is derived, based on the importance of the errors introduced by the outdated flow field relative to those introduced by the sand-transport formulae.

RÉSUMÉ

Un système de modèles destiné à simuler l'évolution sédimentaire générée par la marée est développé, analysé et appliqué. Le système couple un modèle hydrodynamique existant avec un nouveau modèle d'évolution des fonds. Quatre innovations visant à améliorer la précision et l'efficacité du système sont implémentées et testées. D'abord, deux alternatives permettant d'actualiser le champ de vitesse sans tourner le modèle hydrodynamique sont proposées. Ces deux alternatives, basées sur une hypothèse sur le comportement du frottement, sont plus précises que la traditionnelle “correction de continuité”. D'autre part, les résultats du modèle hydrodynamique sont fournis dans le domaine de la fréquence. La synthèse harmonique des séries chronologiques de vitesse simplifie l'interpolation et l'extrapolation des résultats du modèle hydrodynamique et l'utilisation de pas de calcul distincts dans les différentes composantes du système. Ensuite, l'intégration temporelle des flux de sédiments utilise un pas de temps adaptatif, pour réduire le temps de calcul. Finalement, un critère pour déterminer la nécessité d'une nouvelle simulation hydrodynamique est présenté. Le critère est basé sur l'importance des erreurs introduites par le champ de vitesse non actualisé par rapport à celles introduites par les formules de transport de sable.

Keywords: Morphodynamics; tidal inlets; finite volumes; Guadiana estuary.

1 Introduction

Morphodynamic modeling systems are typically composed of different modules for tidal dynamics, wave propagation, sediment transport and bottom updates. These systems are increasingly used to estimate the bathymetric evolution of coastal regions (e.g. Cayocca, 2001; Work *et al.*, 2001), despite their predictive limitations. To some extent, these limitations are associated with the large computational costs required to perform simulations at yearly to decadal time scales, with time steps as low as a few seconds (for the hydrodynamics). To circumvent this problem, accuracy is often sacrificed to reduce computational time (e.g. de Vriend *et al.*, 1993). For instance, these modeling systems often assume that there exists a single “representative

tide” whose effect on the bathymetry is similar to the average effect of the varying tides (e.g. Latteux, 1995). Also, the effect of small bottom changes on the flow field is usually approximated with the “continuity correction”, to reduce the number of calls to the hydrodynamic module. This correction assumes that the depth-integrated current (i.e. the flow discharge per unit width) is unaffected by small bathymetric changes, which can produce unrealistically large velocity estimates for very small depths.

This paper presents the first steps to develop a 2DH coastal area modeling system for long-term morphodynamics, forced only by tides and other low frequency motions. Particular emphasis is placed on the development and analysis of new model reduction techniques, in order to minimize the computational

time and allow long-term predictions. Key features of this modeling system include: (1) alternatives to the continuity correction, to update the velocity field without running the hydrodynamic model, based on assumptions on the behavior of friction; (2) hydrodynamic results provided in the frequency domain to simplify their interpolation and extrapolation; (3) an adaptive time step for the transport module; and, (4) a new criterion to determine when to run the hydrodynamic model. The modeling system is described in Section 2, and validated in Section 3.

2 Modeling system description

2.1 Solution procedure

The general solution procedure is outlined in Fig. 1. On input, the user provides the initial bathymetry. For each morphodynamic time step, sediment fluxes are computed at each element using an empirical formula and integrated in time. A sediment balance equation is then solved to determine the new bathymetry. Before proceeding to a new morphodynamic time step, the flow field is updated through either a new hydrodynamic simulation or a modification of the previous flow field. The choice of the method to update the flow field is based on a criterion deduced below.

2.2 Hydrodynamic module

The hydrodynamic model (ADCIRC – Luettich *et al.*, 1991) solves the fully non-linear depth-averaged shallow-water equations, using linear triangular finite elements and a semi-implicit procedure. The model adopts a Generalized Wave-Continuity Equation approach, which leads to a robust and efficient algorithm (e.g. Kinnmark, 1985). An extensive description of the model and its applications can be found in Luettich and Westerink (2003) and references therein.

ADCIRC can harmonically analyze the model results during the simulation, thereby providing the output in the frequency domain (i.e. nodal amplitudes and phases of elevations and depth-averaged velocities). The evaluation of velocities and elevations through harmonic synthesis in the transport model simplifies their interpolation and allows their extrapolation in time, potentially reducing the length of the hydrodynamic simulations.

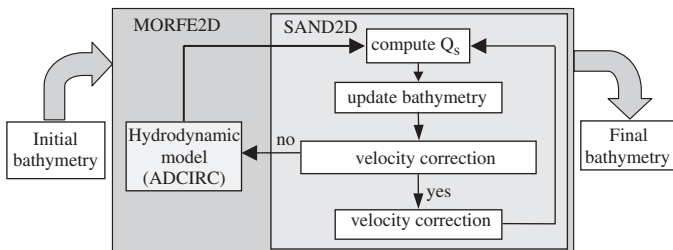


Figure 1 Solution procedure.

2.3 Transport module

The morphodynamics is governed by a depth-integrated sediment conservation equation:

$$\frac{\partial}{\partial t}(cH - (1 - \lambda)h) = -\nabla q_s \quad (1)$$

where t is time, c is the non-dimensional depth-averaged sediment concentration, H is the total water depth, h is the depth relative to a reference level, λ is the porosity, and q_s is the sediment flux. The sand fluxes q_s are evaluated with one of the semi-empirical formulae of Englund and Hansen (1967), Ackers and White (1973), van Rijn (1984a–c) and Karim and Kennedy (1990). Integrating (1) over the simulation time T yields:

$$[cH]_t^{t+T} - (1 - \lambda)\Delta h = -\int_t^{t+T} \nabla q_s dt \quad (2)$$

where Δh is the depth variation. For large values of T (typically several years), the first term on the LHS of Eq. (2) can be neglected. Invoking the Leibnitz rule, the RHS can be rewritten as:

$$-\int_t^{t+T} \nabla q_s dt = -\nabla \int_t^{t+T} q_s dt \quad (3)$$

where the boundary terms were dropped because the limits of integration are space-independent. The depth variation during each morphological time step is therefore given by:

$$\Delta h^i = \frac{1}{1 - \lambda} \nabla Q_s^i \quad (4)$$

where the superscript i indicates the morphological time step, and Q_s^i is the sediment flux integrated over the morphological time step Δt_m^i .

Since the residual fluxes at each morphological time step (Q_s^i) are evaluated separately at each location, each integration can be performed with different intermediate time steps. The use of varying time steps is very useful because q_s varies strongly both in space and in time. The integration is performed with a fourth-order embedded adaptive Runge-Kutta method (Press *et al.*, 1992), in which the time step is automatically adjusted to meet a user-specified criterion. Because the hydrodynamic model results are provided in the frequency domain, velocities at any time step are accurately interpolated through harmonic synthesis.

The general form of a Runge-Kutta algorithm is:

$$Q_s^i(t^n) = Q_s^i(t^{n+1}) + \Delta t \sum_{j=1}^q a_j k_j \quad (5)$$

with:

$$k_j = q_s(t^{n+1} + b_j \Delta t) \quad (6)$$

where a and b are constants that depend on the specific Runge-Kutta method (Press *et al.*, 1992). The time step is dynamically adjusted by comparison between the 5th order and the embedded 4th order truncation error.

The choice of the morphological time step takes advantage of the alternation of flux direction during a tidal cycle. This alternation results in a partial compensation of the ebb and flood fluxes, hence the tide-averaged flux is usually significantly smaller than

the peak fluxes. In order to minimize the variability of Q_s , the morphological time step is thus set equal to an integer number of tidal cycles and is determined through the evaluation of the times of occurrence of high or low water tide at a user-specified node. Therefore, sediment transport computations are performed on a fixed bed throughout the tidal cycle, a simplification valid only if bed changes during this cycle are small.

Preliminary tests suggested that the computational gains associated with using morphodynamic time steps larger than one tidal cycle were modest, and therefore all the simulations presented below use a morphological time step equal to one tidal cycle. However, if the tidal regime is mixed (i.e. diurnal and semi-diurnal signals are similar) taking the morphodynamic time step as an even number of tidal cycles can probably minimize the variability of Q_s , hence improve accuracy.

Bathymetric gradients play an important role in sediment transport. They increase (decrease) the critical shear stress when sediments are moving up-slope (down-slope), acting as a diffusion-like term that stabilizes the numerical simulations. Physically, this effect is considered by modifying the critical shear stress according to the bottom slope along the flow direction (Antunes do Carmo, 1995). Using a node-centered finite volume technique to solve Eq. (4) avoids averaging the bottom slopes, promoting the model stability. In addition, this method guarantees local mass conservation, an important feature at long time scales.

Equation (4) is integrated over node-centered control volumes, defined by the medians of the elements (Fig. 2):

$$\int_{CV} \Delta h^i dV = \frac{1}{1-\lambda} \int_{\Gamma} Q_s^i \cdot \vec{n} d\Gamma \quad (7)$$

where CV indicates the control volume with boundary Γ and \vec{n} is the outward unit normal on Γ . Green's theorem was used to cast the divergence term into a boundary integral. Depths are assumed to vary linearly within each element, while Q_s is assumed constant inside each element and computed at its center.

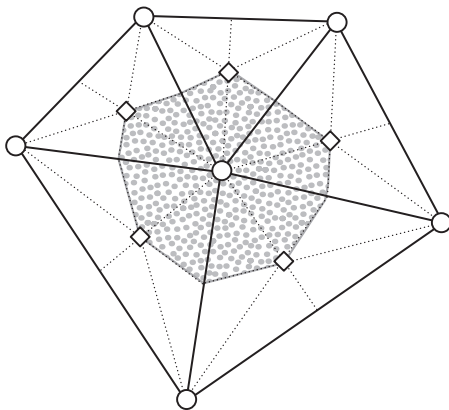


Figure 2 The control volume (shaded area) is defined by the medians (dotted lines) of the elements (solid lines). The circles and squares represent the nodes and element centers, respectively.

2.4 Velocity field update

As the bathymetry evolves, the flow field must be updated accordingly. This update can be achieved in two ways. If the bathymetric changes are “large” (the meaning of this term is discussed below), the flow module has to be run with the new bathymetry; otherwise, velocity corrections can be introduced to update the flow field without running the hydrodynamic model, hence reducing computational costs.

Several models (e.g. Cayocca, 2001) base this velocity correction on the assumption that the water fluxes are only weakly affected by the bathymetric changes. This approach, named the *continuity correction*, is expressed as:

$$(u_k^*, v_k^*) = \frac{H_i}{H_k} (u_i, v_i) = R_c(u_i, v_i) \quad (8)$$

where (u_i, v_i) is the depth-averaged velocity evaluated from ADCIRC results for the bathymetry of the morphodynamic time step i , and the star represents an estimated value for the bathymetry of the morphodynamic step $k > i$. Although this approach is simple and efficient, it produces unrealistically large estimates when H_k becomes very small. Alternative ways to update velocities are therefore sought.

Using both data and a scaling analysis, Friedrichs and Madsen (1992) showed that inertia terms are one to two orders of magnitude smaller than friction in shallow tidal embayments. Neglecting these terms, the momentum equation becomes a balance between friction and the barotropic pressure gradient. Further assuming, like in the continuity correction, that the surface elevation is unaffected by bathymetric changes, the friction term also remains unchanged. Mathematically, this *friction correction* is expressed as:

$$\frac{c_{fk} U_k^* (u_k^*, v_k^*)}{H_k} = \frac{c_{fi} U_i (u_i, v_i)}{H_i} \quad (9)$$

where c_f is the depth-dependent dimensionless friction factor and U is the velocity magnitude. Squaring each side of Eq. (9), it can be solved for the corrected velocities to yield:

$$(u_k^*, v_k^*) = \sqrt{\frac{c_{fi} H_k}{c_{fk} H_i}} (u_i, v_i) = R_f(u_i, v_i) \quad (10)$$

When H_k tends to zero, R_c tends to infinity while R_f tends to zero. For Manning-type friction formulations, $R_f = (H_i/H_k)^{-2/3} = R_c^{-2/3}$. Le Hir *et al.* (2000) used a similar approximation to relate the velocities over tidal flats and in adjacent channels, and verified its accuracy with field data.

As an alternative, the two approximations can be combined into a *mixed continuity-friction correction* by taking an average of the previous two coefficients. The geometric average is used here for its simplicity:

$$R_m = \sqrt{R_c R_f} = \left(\frac{c_{fi} H_i}{c_{fk} H_k} \right)^{1/4} \quad (11)$$

While R_m also tends to infinity when H_k tends to zero, it does so more slowly than R_c .

These three algorithms violate mass conservation, momentum conservation or both. Numerical tests are performed in Section 3

to determine which violation has the least consequences on the prediction of velocities.

2.5 Criterion to determine the adequacy of the velocity correction

When bathymetric changes become “large”, the velocity correction may no longer provide an adequate approximation. A criterion to determine when the velocity correction becomes unacceptable must therefore be established. Considering that the errors introduced by sand transport formulae are large (e.g. Huntley and Bowen, 1989), it is reasonable to impose that those introduced by the velocity correction should be smaller. Denoting the errors introduced by the transport as E , one can write:

$$1/(1 + E) < q_{sn}/q_s < (1 + E) \quad (12)$$

where q_s is the exact sand flux, and q_{sn} is the flux computed with an empirical formula and the correct velocity. This equation can be rewritten as:

$$\begin{cases} (q_{sn} - q_s)/q_s < E & \text{if } q_{sn} > q_s \\ (q_s - q_{sn})/q_s < E/(1 + E) & \text{if } q_{sn} < q_s \end{cases} \quad (13)$$

We therefore impose that:

$$\begin{cases} (\tilde{q}_{sn} - q_{sn})/q_{sn} < \varepsilon & \text{if } \tilde{q}_{sn} > q_{sn} \\ (q_{sn} - \tilde{q}_{sn})/q_{sn} < \varepsilon/(1 + \varepsilon) & \text{if } \tilde{q}_{sn} < q_{sn} \end{cases} \quad (14)$$

where the tilde indicates a flux where the velocity was updated with a velocity correction, and ε is a user-specified constant which represents the maximum acceptable error introduced by the velocity correction. The constant ε should be as large as possible, for computational efficiency, yet small enough to avoid the introduction of significant errors. Considering that sand transport formulae have errors of the order of 100% (van Rijn, 1990), the value of E is about 1. The value of ε should therefore be between 0.1 and 1, a range that will be assessed below.

Noting that sand fluxes are typically proportional to the velocity raised to some power m (with m between 3 and 7, depending on the formula), Eq. (14) can be written:

$$\begin{cases} (R^m U_i^m - U_k^m)/U_k^m < \varepsilon & \text{if } RU_i > U_k \\ (U_k^m - R^m U_i^m)/U_k^m < \varepsilon/(1 + \varepsilon) & \text{if } RU_i < U_k \end{cases} \quad (15)$$

where U_i and U_k are the velocity magnitudes computed with the complete flow model with the old and new bathymetries, respectively, and R is the velocity correction ratio (R_c , R_f or R_m). Equation (15) can be rearranged to yield:

$$\begin{cases} RU_i/U_k < (1 + \varepsilon)^{1/m} & \text{if } RU_i > U_k \\ RU_i/U_k > (1 + \varepsilon)^{-1/m} & \text{if } RU_i < U_k \end{cases} \quad (16)$$

Equation (16) is not readily usable because U_k is unknown *a priori*. A hypothesis on the variation of the velocity with the bathymetry is therefore needed.

The velocity changes with the bathymetry are due to both local and non-local effects, i.e.:

$$U_k = U_i R^* R' \quad (17)$$

where R^* and R' represent the local and non-local effects, respectively. Although little is known about these non-local effects, the

good results provided by the velocity corrections (see Section 3) suggest that: (1) the local effects are generally dominant; and (2) the velocity corrections are good approximations of the local effects (i.e. $R \approx R^*$). If R is larger (smaller) than unity, the dominance of the local effects translates into the product RR' also being larger (smaller) than unity, but smaller (larger) than R^2 :

$$\begin{cases} 1 < RR' < R^2 & \text{if } R > 1 \\ 1 > RR' > R^2 & \text{if } R < 1 \end{cases} \quad (18)$$

Multiplying Eq. (18) by U_i and using Eq. (17):

$$\begin{cases} U_i < U_k < U_i R^2 & \text{if } R > 1 \\ U_i > U_k > U_i R^2 & \text{if } R < 1 \end{cases} \quad (19)$$

Equation (19) can be written as:

$$\begin{cases} 1/R < RU_i/U_k < R & \text{if } R > 1 \\ 1/R > RU_i/U_k > R & \text{if } R < 1 \end{cases} \quad (20)$$

Using Eq. (20), a sufficient condition for Eq. (16) to be verified is therefore:

$$\begin{cases} R < (1 + \varepsilon)^{1/m} & \text{if } R > 1 \\ R > (1 + \varepsilon)^{-1/m} & \text{if } R < 1 \end{cases} \quad (21)$$

Since ε is positive, Eq. (21) reduces to:

$$(1 + \varepsilon)^{-1/m} < R < (1 + \varepsilon)^{1/m} \quad (22)$$

This criterion can be compared with a similar criterion proposed by Latteux (1995) and used by other modeling systems (e.g. Cayocca, 2001; Work *et al.*, 2001):

$$|(H_c - H_i)/H_i| < \varepsilon' \quad (23)$$

where ε' is set to 0.1. Equation (23) can be written as:

$$(1 - \varepsilon')^{-1} > R_c > (1 + \varepsilon')^{-1} \quad (24)$$

For $\varepsilon' = 0.1$, R_c is approximately between 0.9 and 1.1. Taking $R = R_c$ in Eq. (22) with $m = 3$ leads to a ε of 0.3–0.4 (Fig. 3). This value of ε is in the middle of the expected range (0.1–1), confirming the validity of the new approach.

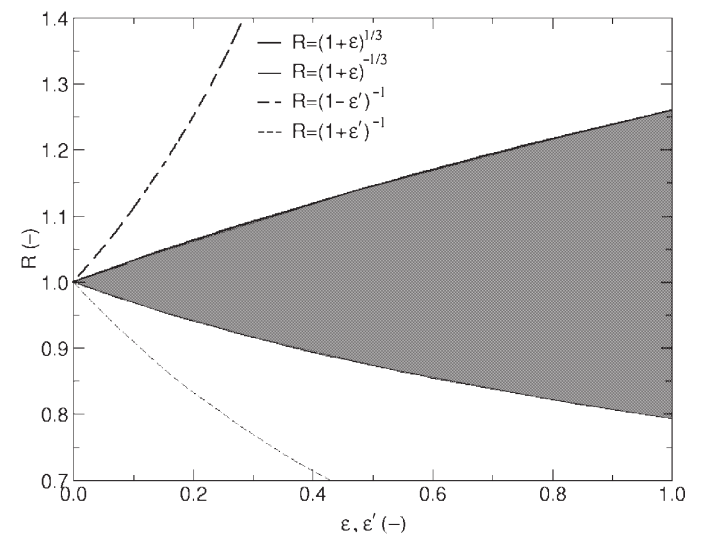


Figure 3 Criterion to determine the adequacy of the velocity correction shown for $m = 3$. The shaded area indicates the acceptable values for R .

2.6 Numerical oscillations

Experience with the modeling system showed that unphysical bathymetric oscillations could develop, a problem reported previously (Jensen *et al.*, 1999; Johnson and Zyserman, 2002). Three features were implemented to address this problem.

First, a weak non-linear filter is applied at every morphodynamic time step to eliminate local extremes in the bathymetry (Fortunato and Oliveira, 2000). A minimum (maximum) occurs for $h_i < h_{\min}$ ($h_i > h_{\max}$), where $h_{\min} = \min\{h_j : j = 1, NEI\}$ ($h_{\max} = \max\{h_j : j = 1, NEI\}$), and NEI is the number of nodes surrounding node i . For each minimum (maximum), h_i and h_{\min} (h_{\max}) are made equal while preserving the volume by setting:

$$h_i^f = h_{\min(\max)}^f = \frac{h_i A_{i\min(\max)} + h_{\min(\max)} A_i}{A_i + A_{i\min(\max)}} \quad (25)$$

where the superscript f indicates a filtered value, and A_i and $A_{i\min(\max)}$ are the areas of the elements surrounding node i and the node where depth is minimum (maximum), respectively. The procedure is repeated until convergence, i.e. until all local extrema have been removed. This filter damps $2\Delta x$ oscillations with minimal introduction of numerical diffusion (Oliveira and Fortunato, 2002a). Stronger filters reported in the literature (Fortunato and Oliveira, 2000; Johnson and Zyserman, 2002) were also tested, but proved to be too diffusive and were abandoned.

Second, finite elements were replaced by finite volumes in the solution of the transport equation. Standard Galerkin finite element formulations of Eq. (4) spatially average either the bed slopes or the sand fluxes at the nodes, thereby reducing the natural diffusive effect of the bed slopes. Finite volume formulations avoid this problem, leading to smoother solutions.

Finally, the possibility of using different grids for flow and sediment transport, a capability justified by the different domain and resolution requirements of the two models, was implemented. The modeler can take advantage of this capability by using a finer grid for transport, to further reduce the oscillations. Small-scale oscillations in the finer grid are dissipated when the bathymetry is mapped to the coarser grid and back for each flow simulation. Although this procedure can potentially lead to mass errors through aliasing and introduce numerical diffusion, the benefits far outweigh the disadvantages.

3 Assessment and application

3.1 Study site

The morphodynamic modeling system is tested in the Guadiana estuary, located at the southern border between Portugal and Spain (Fig. 4). The Guadiana estuary is 76 km long, 70 to 800 m wide and 5 to 15 m deep. The flow is forced mostly by tides and river flow. Tides are semi-diurnal, with ranges between 0.8 and 3.5 m. The river flow enters the estuary mostly from the upstream boundary (Mértola), as the tributaries that reach the estuary are small and their flow controlled by dams. Monthly-averaged river flows vary between 7 and 57 m³/s on average years, and reach 280 m³/s on wet years. Bottom sediments are predominantly sands, with mean diameters of about 600 μm, except near

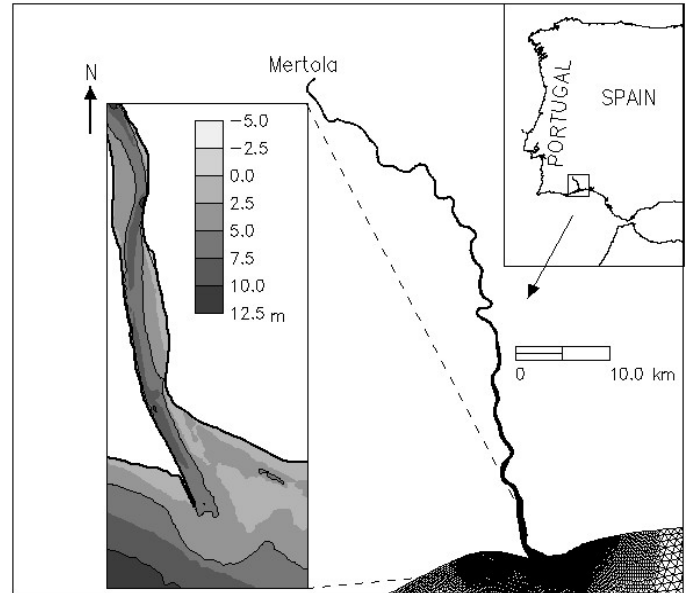


Figure 4 Guadiana estuary: location, grid and bathymetry of the mouth.

the margins where significant amounts of mud are present. The system is strongly flood-dominant because it has few tidal flats (Fortunato *et al.*, 2002b).

The hydrodynamic model was forced by a river flow of 25 m³/s and the major tidal constituent (M_2) taken from the regional model of Fortunato *et al.* (2002a). Major harmonics generated inside the domain (M_4 and M_6) were also included in the harmonic analysis, thus used to force sediment fluxes. The grid has 11,000 nodes, and resolution of the order of 50 m near the mouth. Root mean square elevation errors at four stations are about 10 cm. Further details of the estuarine dynamics and the flow model application and validation are given in Fortunato *et al.* (2002b) and Oliveira and Fortunato (2002b).

The transport grid is generated by taking a subset of the flow grid near the mouth, then splitting each element into four.

3.2 Assessment of the velocity corrections

The ability of the three alternative velocity corrections to predict velocities based on an outdated velocity field was assessed and compared based on results from two simulations with the hydrodynamic model. The first simulation (run A) uses the original bathymetry (A). The second (run B) uses a slightly different bathymetry (B), obtained from bathymetry A through a morphodynamic simulation.

Velocities from the flow model run B during one tidal cycle (U_B) were compared with velocities predicted by each of the three velocity correction schemes (RU_A), using results from run A (U_A) and the two bathymetries. Predictions were only assessed at nodes where bathymetric differences between bathymetries A and B were larger than 1 cm, since elsewhere all the velocity ratios would be almost equal to one.

The comparison indicates that the mixed continuity-friction correction is the most accurate, followed by the friction correction (Fig. 5). The average error (not shown) is always below

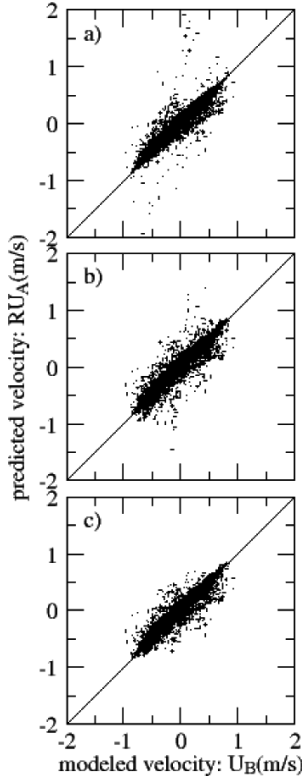


Figure 5 Assessment of the velocity corrections: (a) continuity correction; (b) friction correction; (c) mixed continuity-friction correction.

1 cm/s, showing that all approximations are unbiased. A similar application to a different estuary confirmed these conclusions (Fortunato and Oliveira, 2003), indicating that the results are not fortuitous. The mixed continuity-friction correction is therefore retained hereafter.

3.3 Assessment of the velocity correction criterion

In order to test the criterion to determine when the velocity correction becomes unacceptable, the error associated with the sand transport formulae was estimated by comparing the discrepancies between the bathymetric predictions obtained with different formulae. One-year-long morphodynamic simulations were performed with four different sand transport formulae (van Rijn, 1984a–c; Engelund and Hansen, 1967; Ackers and White, 1973 and Karim and Kennedy, 1990) and a very small value for ε (0.1). This value of the parameter ε should ensure that the error associated with the velocity correction is negligible relative to the one associated to the sand transport formulae. The comparison between these four formulae provides a baseline against which to compare errors associated with larger values of ε , i.e. the difference between the bathymetries obtained with the various transport formulae determines the limit of accuracy achievable by the modeling system.

The discrepancy measure selected to analyze the results was defined as the absolute difference between the elemental depths for each run and a reference run, scaled by the maximum depth variation during the reference simulation, i.e.:

$$D_i = |h_i - h_{ri}| / \max(|\Delta h_{ri}|) \quad (26)$$

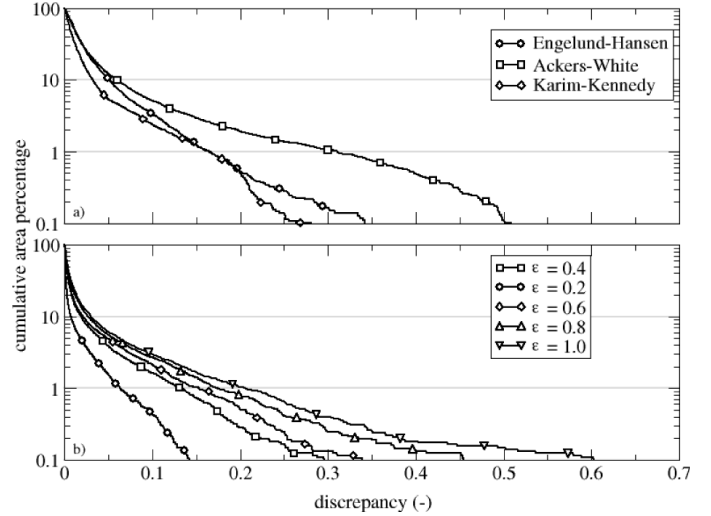


Figure 6 Assessment of the velocity correction criterion: comparison between the errors introduced by the sand transport formulae (a) and the velocity correction (b).

where h_i is the elemental depth predicted by the model for a test simulation, h_{ri} is the prediction for the reference simulation, and Δh_{ri} is the elemental depth variation during the whole reference simulation (with $\max(|\Delta h_{ri}|) = 2.6$ m). The simulation with $\varepsilon = 0.1$ and the van Rijn transport formula was used as reference. These discrepancies were summarized by defining the area of the domain where the discrepancy exceeds a set limit. This results in the cumulative discrepancy distribution curves shown in Fig. 6. Since a large portion of the domain is too deep for any sediment movement to occur, only the elements where bathymetric variations in the reference simulation were larger than 1 cm were considered.

The discrepancies associated with the velocity correction are similar to those associated with the sand transport formulae for $\varepsilon = 1.0$, and decrease roughly proportionally with ε . The number of calls to the hydrodynamic model grows roughly linearly with this parameter. In practice, the choice of ε should therefore depend on the acceptable accuracy, and on the computational costs. In the following simulations, ε is taken as 0.5.

3.4 Application

The modeling system is used to reproduce qualitatively the expected behavior of the Guadiana mouth. It is generally accepted that the tidal prism (P) and the minimum cross-sectional area (A) of a stable tidal inlet are related as:

$$A = CP^n \quad (27)$$

where C and n have been determined empirically by several authors for various types of inlets (e.g. Jarrett, 1976). These two parameters depend on various factors. For instance, the cross-sectional area is smaller in coasts with a strong littoral drift, or in unjettied inlets, as the wave action promotes accretion. Therefore, a morphodynamic simulation of the Guadiana mouth without considering waves should lead to a larger equilibrium cross-sectional area. Also, it has been shown analytically that C grows

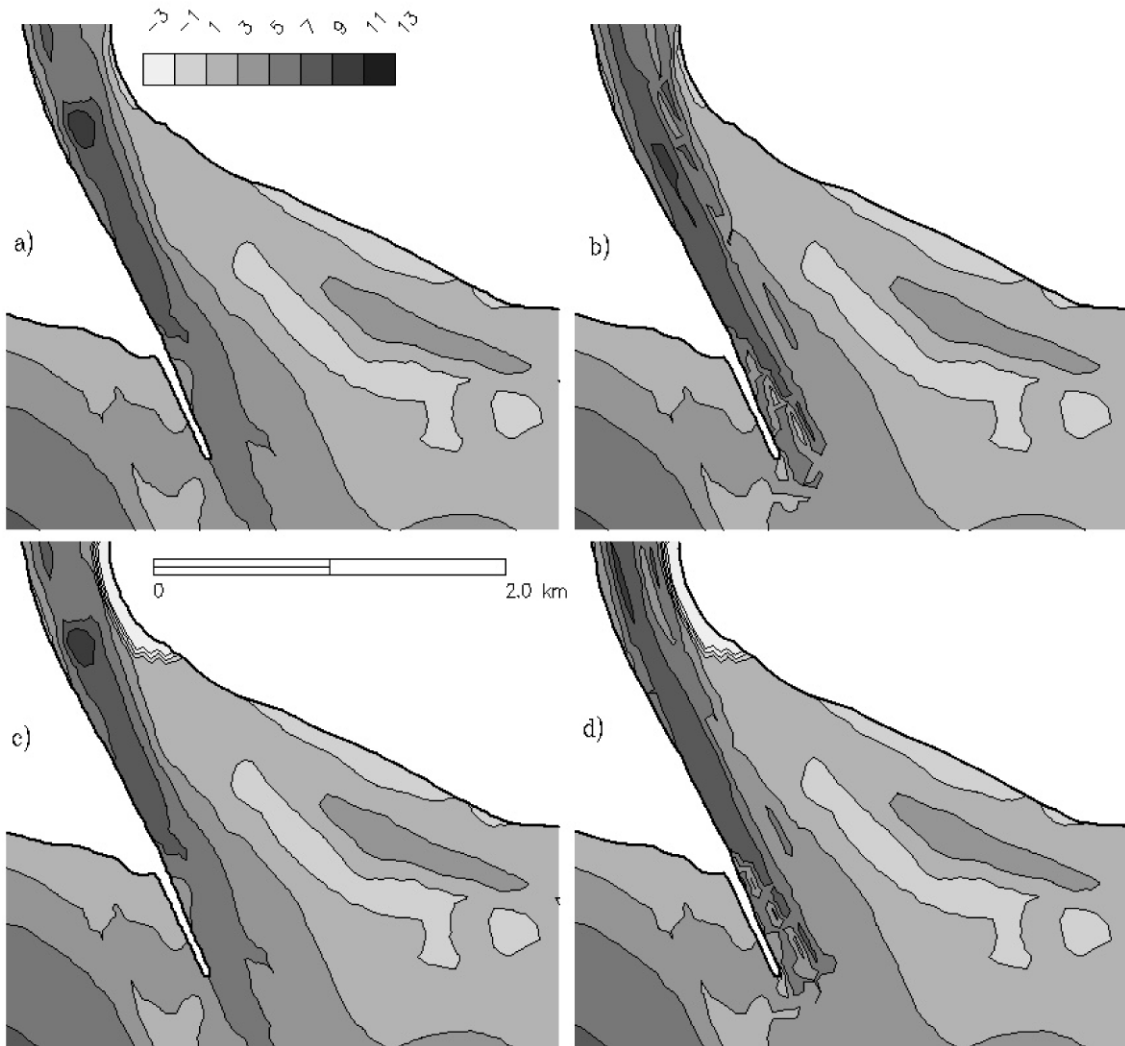


Figure 7 Bathymetry of the Guadiana estuary mouth, color-shaded in meters: initial conditions (a, c) and model predictions after a three-year simulation (b, d). In the lower panels, the inlet width was partially reduced with a fixed structure.

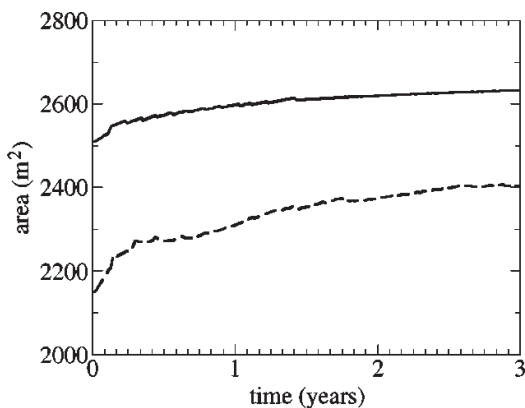


Figure 8 Time evolution of the average cross-section for the original bathymetry (solid line) and the narrowed inlet (dashed line).

weakly with the inlet width (Kraus, 1998; Hughes, 2002). Therefore, reducing the inlet width should lead to a smaller equilibrium cross-sectional area.

This behavior was verified in two three-year-long morphodynamic simulations. In the first simulation, the real bathymetry of the estuary was used; in the second, the estuary width was locally

reduced (Fig. 7). The cross-sectional area in the narrowest section of the estuary, monitored during the simulation, exhibits the expected behavior (Fig. 8): the area increases in both cases, but tends to a larger value in the first simulation.

4 Conclusions

The modeling system for tidally driven morphodynamics introduced herein includes some innovations that can easily be introduced in similar systems.

Providing hydrodynamic model results in the frequency domain allows for their straightforward extrapolation and interpolation in time. The extrapolation can improve computational efficiency by reducing the duration of the hydrodynamic simulations, while the interpolation is useful if the time steps of the flow and the sand transport models differ. In particular, this occurs when the transport model uses an adaptive time step to improve computational efficiency, an approach whose feasibility was also demonstrated herein.

Also, the present modeling system incorporates a new criterion to determine when to run the hydrodynamic model. Although in

practice this criterion differs little from an existing empirical one, it offers a clearer understanding of how the choice of its parameter ε can affect the final results. In addition, the new criterion shows that the higher the exponents of velocity in the sediment flux expressions, the lower the limits of validity of the outdated flow field. This relationship indicates that sensitivity to errors in the velocity field increases with the velocity exponents in the sediment transport formulae.

Finally, the two new velocity corrections to estimate changes in the velocity field associated with small bottom variations were shown to be superior to the traditional continuity correction. In particular, the mixed continuity-friction correction reduced the maximum velocity error by 75% relative to the previous approach. The violation of water mass continuity by the two new velocity corrections does not appear to have negative consequences when sediment fluxes are computed with empirical formulae, such as was done herein. However, if these fluxes are computed through the solution of a transport equation, the flow mass errors may generate sediment mass imbalances (Oliveira *et al.*, 2000). Also, the arguments used to justify the friction correction suggest that this method should be the most appropriate in friction-dominated areas, whereas the continuity correction could be optimal in deeper areas. Although attempts to determine criteria do decide the best velocity correction as a function of the local conditions proved inconclusive, this issue remains open.

Acknowledgements

This work was sponsored by the *Laboratório Nacional de Engenharia Civil*, project *Morfodinâmica de Barras*. We thank R.A. Luettich, Jr. and W.W. Westerink for the model ADCIRC, A.M. Baptista for the software used to produce Figs. 4 and 8, Mr. J.P. Fernandes for his assistance with the C-shell language and three anonymous reviewers for excellent suggestions.

Notations

A [m²] = minimum equilibrium cross-sectional area of an inlet
 CV = control-volume
 c [–] = depth-averaged sediment concentration
 c_f [–] = friction factor
 E [–] = relative error in the sediment fluxes introduced by the empirical formulae
 H [m] = total water depth
 h [m] = depth relative to a reference level
 \vec{n} = outward unit normal on the control volume
 P [m³] = tidal prism
 Q_s^i [m²] = sediment flux integrated over a morphological time step
 q_s [m²/s] = instantaneous sediment flux
 R [–] = velocity correction ratio
 T [s] = duration of the simulation
 t [s] = time

U [m/s] = depth-averaged velocity magnitude
 (u, v) [m/s] = depth-averaged velocity
 (u^*, v^*) [m/s] = estimate of the depth-averaged velocity
 Δh [m] = depth variation
 ε [–] = maximum acceptable error introduced by the velocity correction
 Γ = boundary of the control volume
 λ [–] = porosity

References

1. ACKERS, P. and WHITE, W.R. (1973). "Sediment Transport: A New Approach and Analysis", *J. Hyd. Div.*, 99, 2041–2060.
2. ANTUNES DO CARMO, J.S. (1995). *Contribuição para o estudo dos processos morfodinâmicos em regiões costeiras e estuarinas*. Ph.D. Dissertation, Univ. Coimbra, Coimbra, Portugal, 225 pp (in Portuguese).
3. CAYOCCA, F. (2001). "Long-Term Morphological Modeling of a Tidal Inlet: The Arcachon Basin, France", *Coastal Engrg.*, 42, 115–142.
4. DE VRIEND, H.J., CAPOBIANCO, M., CHESTER, T., DE SWART, H.E., LATTEUX, B. and STIVE, M.J.F. (1993). "Approaches to Long-Term Modeling of Coastal Morphology: A Review", *Coast. Eng.*, 21, 225–269.
5. ENGELUND, F. and HANSEN, F. (1967). *A monograph of sediment transport in alluvial channels*, Teknisk Forlag, Copenhagen, Denmark.
6. FORTUNATO, A.B., and OLIVEIRA, A. (2000). "On the Representation of Bathymetry by Unstructured Grids", L.R. Bentley *et al.* (eds), *Computational Methods in Water Resources XIII*, Balkema, Vol. 2, 889–896.
7. FORTUNATO, A.B., PINTO, L.L., OLIVEIRA, A. and FERREIRA, J.S. (2002a). "Tidally-Generated Shelf Waves Off the Western Iberian Coast", *Cont. Shelf Res.*, 22(14), 1935–1950.
8. FORTUNATO, A.B., OLIVEIRA, A. and ALVES, E. (2002b). "Circulation and Salinity Intrusion in the Guadiana Estuary", *Thalassas*, 18(2), 43–65.
9. FORTUNATO, A.B., and OLIVEIRA, A. (2003). "Modeling Estuarine Morphodynamics Using Unstructured Grids", J.I. Barbosa (ed.), *VII Congresso de Mecânica Aplicada e Computacional*, Universidade de Évora, Vol. 4, 2027–2036 (in Portuguese).
10. FRIEDRICHS, C.T. and MADSEN, O.E. (1992). "Nonlinear Diffusion of the Tidal Signal in Frictionally Dominated Embayments", *J. Geophys. Res.*, 97(C4), 5637–5650.
11. HUGHES, S.A. (2002). "Equilibrium Cross Sectional Area at Tidal Inlets", *J. Coast. Res.*, 18(1), 160–174.
12. HUNTLEY, D.A. and BOWEN, A.J. (1989). "Modeling Sand Transport on Continental Shelves", A.M. Davies (ed.), *Modeling Marine Systems*, CRC Press, 221–254.
13. JARRETT, J.T. (1976). *Tidal Prism – Inlet Area Relationships*. GITI Report 3, US Army Engineer Waterways Experiment Station, Vicksburg, Mississippi.

14. JENSEN, J.H., MADSEN, E.O. and FREDSOE, J. (1999). "Oblique Flow Over Dredged Channels: II. Sediment Transport and Morphology", *J. Hydr. Engrg.*, 125(11), 1190–1198.
15. JOHNSON, H.K. and ZYSERMAN, J.A. (2002). "Controlling Spatial Oscillations in Bed Level Update Schemes", *Coast. Eng.*, 46, 109–126.
16. KARIM, M.F. and KENNEDY, J.F. (1990). "Menu of Couple Velocity and Sediment Discharge Relation for Rivers", *J. Hydr. Engrg.*, 116(8).
17. KINNMARK, I.P.E. (1985). *The Shallow Water Equations: Formulation, Analysis and Application*. In: C.A. Brebia and S.A. Orszag (eds.), *Lecture Notes in Engineering*, 15, Springer-Verlag, Berlin, 187 pp.
18. KRAUS, N.C. (1998). "Inlet Cross-Section Area Calculated by Process-Based Models", *26th International Coastal Engineering Conference*, Vol. 3, pp. 3265–3278.
19. LATTEUX, B. (1995). "Techniques for Long-Term Morphological Simulation under Tidal Action", *Mar. Geol.*, 126(1–4), 129–141.
20. LE HIR, P., ROBERTS, W., CAZAILLET, O., CHRISTIE, M., BASSOULLET, P. and BACHER, C. (2000). "Characterization of Intertidal Flats Hydrodynamics", *Cont. Shelf Res.*, 20(12–13), 1433–1459.
21. LUETTICH, R.A., WESTERINK, J.J. and SHEFFNER, N.W. (1991). *ADCIRC: An Advanced Three-Dimensional Model for Shelves, Coasts and Estuaries. Report 1: Theory and Methodology of ADCIRC-2DDI and ADCIRC-3DL*, Department of the Army, US Army Corps of Engineers.
22. LUETTICH, R.A. and WESTERINK, J.J. (2003). [Http://www.marine.unc.edu/C_CATS/adcirc/document/ADCIRC_main_frame.html](http://www.marine.unc.edu/C_CATS/adcirc/document/ADCIRC_main_frame.html), web site.
23. OLIVEIRA, A. and FORTUNATO, A.B. (2002a). "Towards an Oscillation-Free, Mass Conservative, Eulerian-Lagrangian Transport Model", *J. Comp. Phys.*, 183(1), 142–164.
24. OLIVEIRA, A. and FORTUNATO, A.B. (2002b). "Oscillation-Removal Schemes for Salinity Studies", M.L. Spaulding (ed.), *Estuarine and Coastal Modeling VII*, ASCE, 501–518.
25. OLIVEIRA, A., FORTUNATO, A.B. and BAPTISTA, A.M. (2000). "Mass Balance in Eulerian-Lagrangian Transport Simulations in Estuaries", *J. Hydr. Engrg.*, 126(8), 605–614.
26. PRESS, W.H., TEUKOLSKY, S.A., VETTERLING, W.T. and FLANNERY, B.P. (1992). *Numerical Recipes in Fortran*, Cambridge University Press, New York.
27. VAN RIJN, L.C. (1984a). "Sediment Transport – Part 1: Bed Load Transport", *J. Hydr. Engrg.*, 110(10), 1431–1456.
28. VAN RIJN, L.C. (1984b). "Sediment Transport – Part 2: Suspended Load Transport", *J. Hydr. Engrg.*, 110(11), 1613–1641.
29. VAN RIJN, L.C. (1984c). "Sediment Transport – Part 3: Bed Forms and Alluvial Roughness", *J. Hydr. Engrg.*, 110(12), 1733–1754.
30. VAN RIJN, L.C. (1990). *Handbook of Sediment Transport by Currents and Waves*, Report H 461, Delft Hydraulics, Delft, The Netherlands.
31. WORK, P.A., GUAN, J., HAYTER, E.J. and ELÇI, S. (2001). "Mesoscale Model for Morphologic Change at Tidal Inlets", *J. Waterw. Port Coast. Ocean Eng.*, 127(5), 282–289.